



RESEARCH LETTER

10.1002/2017GL075552

Key Points:

- TGF afterglows are predicted as a new thunderstorm radiation mechanism, next to TGFs and gamma ray glows
- TGF afterglows produce a relocated and prolonged detectable signal, from intermediate neutrons
- TGF afterglows might have been observed by Gurevich et al. in 2011

Correspondence to:

C. Rutjes,
casper.rutjes@cwil.nl

Citation:

Rutjes, C., Diniz, G., Ferreira, I. S., & Ebert, U. (2017). TGF afterglows: A new radiation mechanism from thunderstorms. *Geophysical Research Letters*, 44, 10,702–10,712. <https://doi.org/10.1002/2017GL075552>

Received 19 APR 2017

Accepted 27 SEP 2017

Accepted article online 2 OCT 2017

Published online 21 OCT 2017

TGF Afterglows: A New Radiation Mechanism From Thunderstorms

C. Rutjes¹, G. Diniz², I. S. Ferreira², and U. Ebert^{1,3}

¹Centrum Wiskunde & Informatica (CWI), Amsterdam, Netherlands, ²Instituto de Física, Universidade de Brasília, Brasília, Brazil, ³Department of Applied Physics, Eindhoven University of Technology, Eindhoven, Netherlands

Abstract Thunderstorms are known to create terrestrial gamma ray flashes (TGFs) which are microsecond-long bursts created by runaway of thermal electrons from propagating lightning leaders, as well as gamma ray glows that possibly are created by relativistic runaway electron avalanches (RREA) that can last for minutes or more and are sometimes terminated by a discharge. In this work we predict a new intermediate thunderstorm radiation mechanism, which we call TGF afterglow, as it is caused by the capture of photonuclear neutrons produced by a TGF. TGF afterglows are milliseconds to seconds long; this duration is caused by the thermalization time of the intermediate neutrons. TGF afterglows indicate that the primary TGF has produced photons in the energy range of 10–30 MeV; they are nondirectional in contrast to the primary TGF. Gurevich et al. might have reported TGF afterglows in 2011.

Plain Language Summary Thunderstorms are known to create high-energy radiation, such as short flashes of gamma rays called terrestrial gamma ray flashes (TGFs) and long duration gamma ray glows. Whereas TGFs are the result of the developing lightning discharge, lightning is observed to terminate the usual gamma ray glows. In this work we predict a new intermediate thunderstorm radiation mechanism, which we call TGF afterglow. It is causally related to a TGF as it is formed by intermediate neutrons generated in the TGF through the photonuclear interaction. It is of intermediate duration, longer than the microsecond fast TGF and faster than the seconds to minutes long gamma ray glow. We show, by means of Monte Carlo simulations, that TGF afterglows produce detectable signals above the cosmic ray background. TGF afterglows might have been observed by Gurevich et al. in 2011.

1. Introduction

Thunderstorms emit energetic radiation of different types. Best known are Terrestrial Gamma ray Flashes (TGFs) which are microsecond-long bursts of photons that were first observed from space (Briggs et al., 2010; Fishman et al., 1994); they can be accompanied by bursts of electron positron pairs (Briggs et al., 2011; Dwyer, Grefenstette, et al., 2008). On the other hand, gamma ray glows last much longer, for minutes or even hours; they have been observed on ground, from balloons and aircraft (Adachi et al., 2008; Chilingarian et al., 2010, 2011; Eack et al., 1996; McCarthy & Parks, 1985; Torii et al., 2002; Tsuchiya et al., 2007;). Chilingarian et al. call them thunderstorm ground enhancements, which refers to the fact that the detector is located on ground.

The different properties of flashes and glows have been related to different physical mechanisms. TGFs originate from cold runaway (Gurevich, 1961) where thermal electrons accelerate to tens of MeV in the strong electric fields of a propagating leader discharge. TGFs appear in bursts that last for microseconds to milliseconds with a temporal distribution sketched in Figure 1; they correlate with leader propagation. Researchers have investigated how the streamer phase (Chanrion & Neubert, 2010; Köhn et al., 2016; Li et al., 2009; Moss et al., 2006) or the leader phase (Celestin & Pasko, 2011; Celestin et al., 2012; Chanrion et al., 2014; Köhn et al., 2014; Köhn & Ebert, 2015) could accelerate electrons to energies that could explain the gamma rays as an effect of bremsstrahlung. Experimentally cold runaway has been found in pulsed discharges (Kostyrya et al., 2006; Shao et al., 2011; Tarasenko et al., 2008) and during the formation of meter long laboratory sparks (Cooray et al., 2009; Dwyer, Saleh, et al., 2008; Kochkin et al., 2012, 2015, 2016; Nguyen et al., 2008; Noggle et al., 1968; Rep'ev & Repin, 2008). Glows, on the other hand, would originate from relativistic runaway electron avalanches (RREA) (Dwyer, 2003; Gurevich et al., 1992), with feedback of photons and positrons creating new avalanches (Babich et al., 2005; Dwyer, 2007, 2012); they evolve on the time scale of seconds to minutes

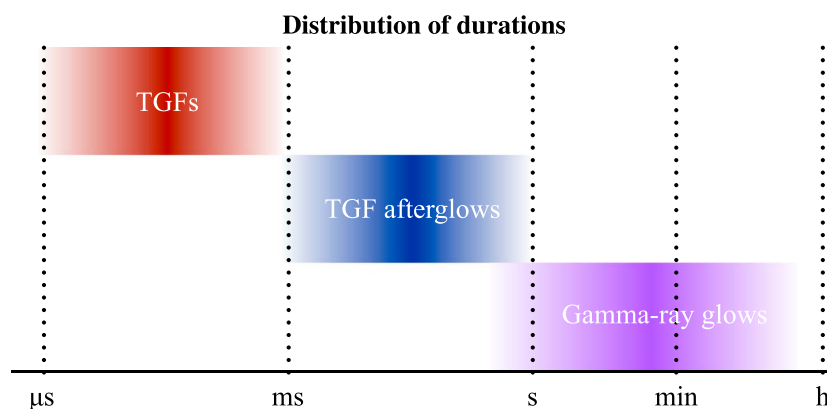


Figure 1. Sketch of the distribution of durations of TGFs, TGF afterglows, and gamma ray glows.

and even hours, as sketched in Figure 1 as well. Whereas lightning leaders produce TGFs, lightning is observed to terminate gamma ray glows (Chilingarian et al., 2015; Kelley et al., 2015; McCarthy & Parks, 1985).

Here we predict a new intermediate thunderstorm radiation mechanism, which we call TGF afterglow, that evolves on the time scale of milliseconds to seconds, as also sketched in Figure 1. In short, when photons in the TGF are energetic enough to release neutrons from air molecules by a photonuclear reaction, the neutrons have initial energies of tens of MeV and slowly cool down through collisions with nuclei of air molecules (as neutrons have no electric charge). During thermalization they can be captured again by nuclei and sometimes with the release of a high-energy photon, hence, in those cases reverting the photonuclear reaction.

That thunderstorms produce neutrons is observed (Bratolyubova-Tsulukidze et al., 2004; Chilingarian et al., 2012; Gurevich et al., 2012; Gurevich et al., 2015; Kozlov et al., 2013; Shah et al., 1985; Shyam & Kaushik, 1999; Starodubtsev et al., 2012; Toropov et al., 2013) and the relevant generation channels have been identified (Babich, 2006; Babich & Roussel-Dupré, 2007; Babich, 2007; Babich et al., 2014; Fleischer et al., 1974) as photonuclear reactions $\gamma + {}^{14}\text{N} \rightarrow n + {}^{13}\text{N}$, $\gamma + {}^{16}\text{O} \rightarrow n + {}^{15}\text{O}$, and $\gamma + {}^{40}\text{Ar} \rightarrow n + {}^{39}\text{Ar}$, with threshold energies of $\epsilon_N = 10.55$ MeV, $\epsilon_O = 15.7$ MeV, and $\epsilon_{Ar} = 9.55$ MeV, respectively (Dietrich & Berman, 1988). The photonuclear cross section is maximal for photons of roughly 23 MeV, creating neutrons of roughly 13 MeV; for a further discussion of the energy spectrum of the neutrons, we refer to Babich et al. (2010). Electrodisintegration reactions (where electrons react with nuclei) could contribute to neutron generation as well, but their contribution is negligible (Babich et al., 2014). The simulations by Babich et al. (2007, 2008), Carlson et al. (2010), Drozdov et al. (2013), and Köhn and Ebert (2015) have focused on neutron production from TGFs, with the number of neutrons produced by a typical TGF varying from 10^{12} neutrons by Carlson et al. (2010) to 10^{15} neutrons by Babich et al. (2007, 2008). This is mainly due to different assumptions of the total number of photons and their spectrum, or of the initial electrons that create the photons by bremsstrahlung. These studies focus on the neutron emission, and we will return to them in section 2. The present study addresses for the first time the prolonged and relocated gamma ray glow generated by the nuclear capture of the neutrons during their thermalization.

Gurevich et al. (2011) have recently observed gamma ray emissions lasting 100 to 600 ms during lightning activity, with some inner temporal structures with durations that are too long for a TGF, which on ground maximally lasts a few hundreds of microseconds. These observations might be the first measurement of TGF afterglows. We will return to these observations in section 3 to illustrate how TGF afterglows would qualitatively appear in measurements.

2. Simulations

2.1. Setup of Simulations

Here we present two simulations made with the general purpose Monte Carlo code FLUKA [www.fluka.org] (Böhlen et al., 2014; Ferrari et al., 2005), which performs very well in the energy regime relevant for TGFs (Rutjes et al., 2016), and which has state-of-the-art neutron transport and interactions (Böhlen et al., 2014). We simulate in air (78.085% N_2 , 20.95% O_2 , and 0.965% Ar) with the altitude-dependent density profile given by the "U.S. Standard Atmosphere (1976)" (by the U.S. Committee on Extension to the Standard Atmosphere).

We perform both simulations within a cylindrical section of the atmosphere extending from ground up to 18 km altitude, with a radius of 12 km. Within FLUKA, this volume is partitioned into 72 horizontal slabs of 250 m thickness in altitude. Every slab is filled with a homogenous air density determined by the air density of the U.S. Standard Atmosphere (1976) at the bottom of each slab, resulting in an exponential density profile starting from 1.225 kg m^{-3} in the lowermost slab up to 0.1216 kg m^{-3} in the uppermost slab. The temperature, however, is constant and equal to 293 K everywhere. Each horizontal slab interface acts as an infinitely thin virtual detector, which detects any passing particle. The output that we record at these interfaces is as follows: the particle type and its kinetic energy, its position in the interface plane, and the time of passing.

The output allows to calculate directly the average flux through the interfaces within a time bin. The time bins are equally spaced on logarithmic scale, with edges given by 10^p s , where p ranges from -9 to 2 in steps of 0.1 . The particle density at the interfaces is approximated by dividing the flux by the velocity; more precisely, for the neutrons we add the inverse square root of the kinetic energy of all particles passing the interface within a time bin with an appropriate factor ($\sqrt{m_n/2}$). This approximation of the density is within the accuracy level of other parameters. This time-averaged density is presented in different manners in Figures 2 and 3. The top panel shows these averaged densities integrated over the horizontal interfaces as a function of the discrete altitudes of these interfaces. The middle panel shows the average density as a function of radius at a given altitude. The bottom panel shows the total particle numbers in the system. Discretization artifacts in these figures are due to the discreteness of the interface altitudes and the time bins.

After the primary electron acceleration in a discharge, electrons, photons, neutrons, and other TGF products move independently through the atmosphere colliding only with neutral gas molecules, hence the further evolution is linear. We therefore always start with 10^8 particles, and we can get higher particle numbers by multiplying initial, intermediate and final states by the same number. The number 10^8 is chosen as a compromise between statistical accuracy and computational demands.

As already discussed, electrons can gain high energies near leader discharges, and these electron energies are converted into photons by bremsstrahlung. A recent study by Mailyan et al. (2016) of 46 TGFs constrains the average number of electrons with energies above 1 MeV to approximately 2×10^{18} , with a range from 4×10^{16} to 3×10^{19} , for source altitudes above 10 km. According to Briggs et al. (2010) and Marisaldi et al. (2014), photon energies can reach up to tens of MeV. We here concentrate on the photons with energies between 10 and 30 MeV, as they can create neutrons by a photonuclear interaction. Gjesteland et al. (2015) analyze three TGFs and estimate that the number of photons with energy above 1 MeV varies between 10^{17} and 10^{20} under the assumption that the TGFs have started at 8 km altitude.

2.2. TGF Afterglow Generated by the Primary TGF

Our first simulation assumes that the TGF is at 8 km altitude and directed downward. It starts with 10^8 photons with uniformly distributed energies between 10 and 30 MeV. Using the results of Gjesteland et al. (2015), and assuming that 1% of the photons with energy above 1 MeV have an energy above 10 MeV, we should actually consider $10^{16 \pm 1}$ photons above 10 MeV rather than 10^8 . But as the evolution outside the TGF source is linear, we can take this into account by multiplying the result of the evolution of 10^8 photons by a factor $10^{8 \pm 1}$.

Figure 2 shows the evolution as function of the logarithm of time. Photons are included only if their energy exceeds 10 keV. The presented quantities are defined in section 2.1. Figure 2 (top), viewed from left to right, shows first the light cone of the developing TGF as nonfilled red to yellow contours. Photons moving upward have been backscattered or they are secondary, which implies that they have lost a significant amount of energy. Therefore, only the primary photons (that move downward), will be energetic enough to produce neutrons; hence, the neutron cloud appears only at lower altitudes in this configuration. The mean free path of the photonuclear reaction scales with density as $\ell = \ell_0 \frac{\rho_0}{\rho}$. For the integrated density (starting at 8 km downward), the mean free path of the photonuclear cross section equals 5 km, consistent with Figure 2.

When the neutrons are just created, their typical energy is of the order of 13 MeV (the energy of the maximum of the photonuclear cross section minus the neutron-binding energy in nitrogen nuclei); then the neutrons diffuse isotropically and cool down (the neutron energy is given in Figure 2, bottom). While cooling down, the intermediate neutrons do create some photons by inelastic scattering, visible in Figure 2 (top) at around 3 km, where the TGF envelope extends longer in time than at other altitudes, but after 10^{-4} s the secondary photons produced by inelastic scattering have energies below 10 keV and are thus not shown. The time for

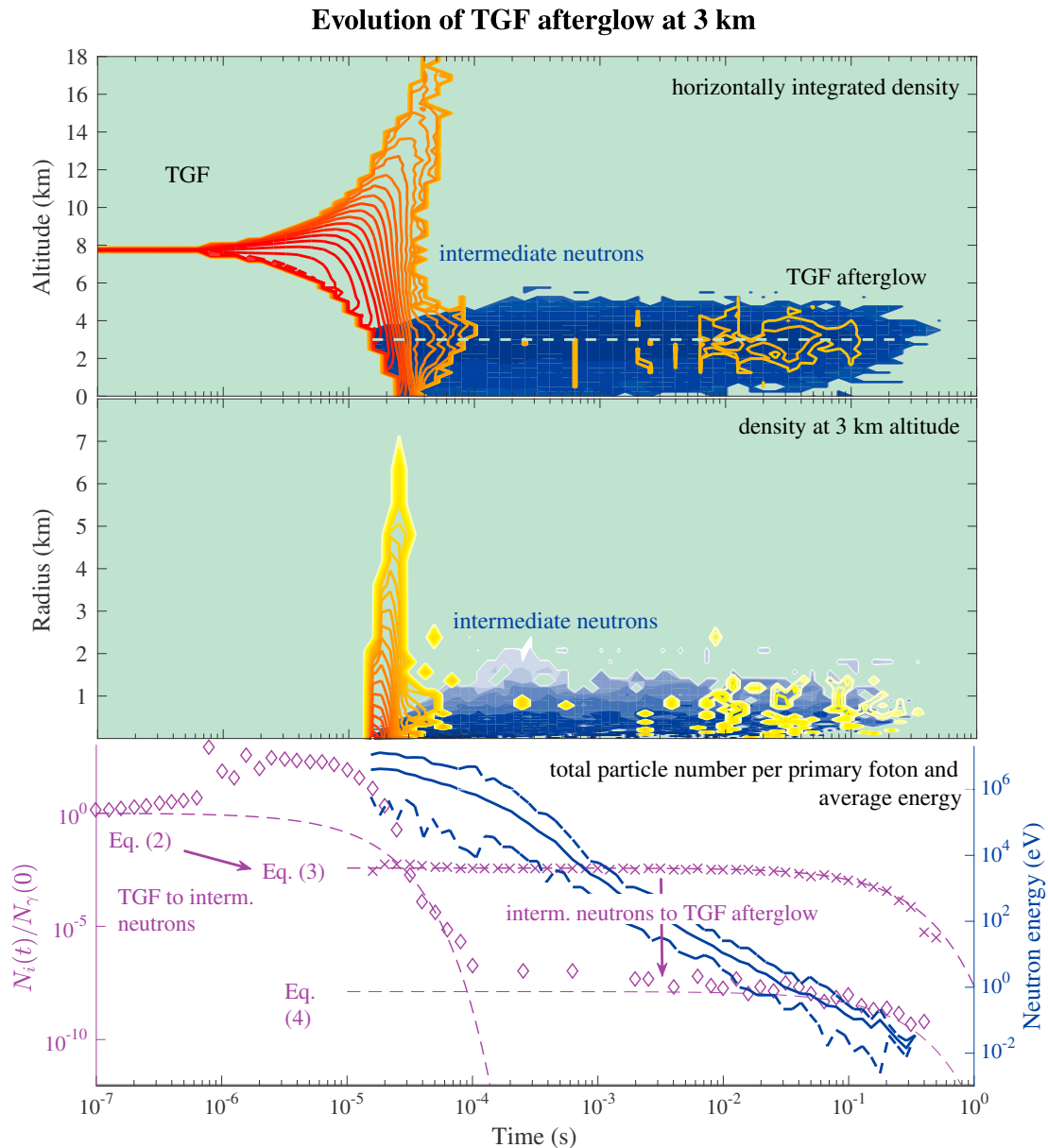


Figure 2. Evolution of the TGF afterglow generated by the primary TGF as a function of the logarithm of time. (top and middle) Contour figures of the photon and neutron density (see definitions in section 2.1), on a logarithmic scale; contours represent half a decade (i.e., a factor of $10^{0.5}$). The contour lines (red, yellow to white) are photons above 10 keV, the filled contours (blue to white) are neutrons. In Figure 2 (top) the density is horizontally integrated. Figure 2 (middle) gives the density profile as a function of radius at 3 km altitude, the density is averaged over rings around the symmetry axis. (bottom) Two quantities: on the left y axis in purple, the total particle number $N_i(t)$ of photons (diamonds) and neutrons (crosses), per initial photon $N_\gamma(0)$, with their approximations given by equations (2)–(4); on the right y axis in blue, the average neutron energy is drawn as a solid line, together with the minimal and the maximal neutron energy as dashed lines.

neutron thermalization scales as $t = t_0 \frac{n_0}{n}$. We see in Figure 2 (bottom) that around 3 km altitude the intermediate neutrons take 0.5 s to thermalize. Neutrons can (at any energy) be captured again, but the cross section for neutron capture increases for decreasing energy as $\sigma_{\text{capture}} \propto 1/\sqrt{E_{\text{neutron}}} \propto 1/v_{\text{neutron}}$, according to the so-called $1/v$ law (see chapter II of Blatt & Weisskopf, 1979). Because of the $1/v$ law, the rate k_{capt} of neutron capture and hence of photon production in the TGF afterglow is constant for constant air density, as $k_{\text{capt}} = v_{\text{neutron}} \sigma_{\text{capture}} n_{\text{air}} \propto \frac{n}{n_0}$. Actually, the most significant capture pathway is not producing a high-energy photon, but of radiocarbon (i.e., $n + {}^{14}\text{N} \rightarrow {}^{14}\text{C} + p$). The cross section for this reaction is $\sigma_{\text{capt}} = 1.8 \times 10^{-28} \text{ m}^2$

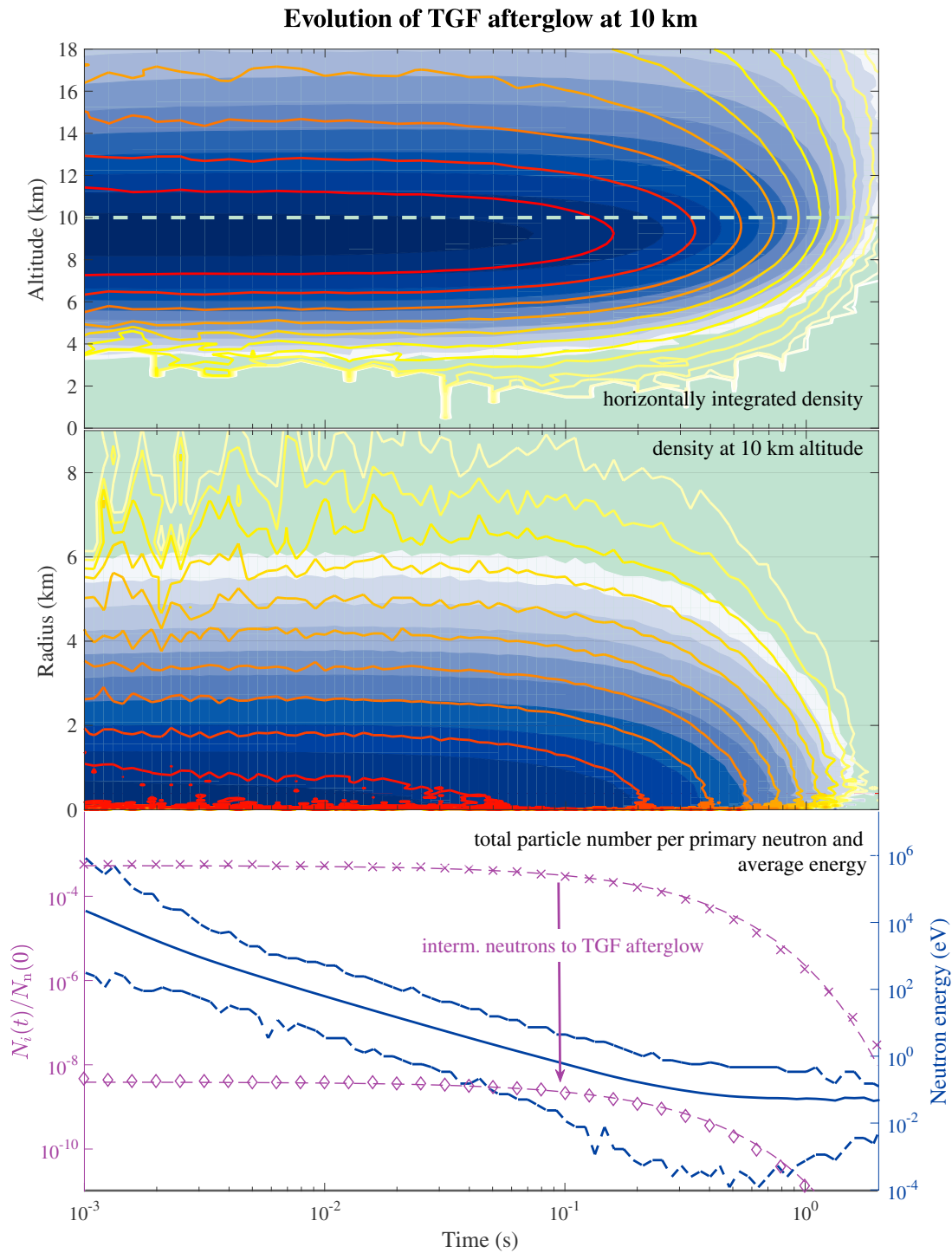


Figure 3. The same as in Figure 2, but now for the TGF afterglow that started from a neutron source at 10 km directed downward. In this figure time is plotted only from 10^{-3} s onward, focusing on the TGF afterglow. Figure 3 (bottom) does not represent the total particle number as some escaped out of the system at the upper boundary at 18 km, see text. The decay rates, that is, the fits of the purple dashed lines, are the same as in Figure 2, adapted to the lower air density (at 10 km compared to 3 km).

(Choi et al., 2007) at thermal velocities (0.025 eV, 2200 m/s), yielding a neutron capture rate of $15.8 \text{ s}^{-1} \frac{n}{n_0}$. The TGF afterglow time scale is thus

$$T_{\text{afterglow}} = 1/k_{\text{capt}} \approx 0.063 \text{ s} \exp\left(\frac{h}{7 \text{ km}}\right), \quad (1)$$

if one assumes an exponential air density profile with a scale height of 7 km.

Figure 2 (bottom) shows the total number of photons and neutrons. This number is the domain-integrated time-averaged density, as explained in section 2.1. The evolution can be explained in a simple way, with three species and four rates, where we for convenience neglect the altitude (i.e., air density) dependence of the reaction rates (as all frequencies scale as $f = f_0 \frac{n}{n_0}$). The first reaction is the absorption of high-energy photons,

$$N_\gamma(t) \approx N_\gamma(0) \exp[-k_{\text{ph-absorp}} t] \quad (2)$$

with the photon absorption rate $k_{\text{ph-absorb}} = \mu c \approx 2 \times 10^5 \text{ s}^{-1}$ at STP, (where μ is the photon attenuation coefficient; for a discussion see Rutjes et al., 2016). The loss due to the production of neutrons, that is, the photonuclear reaction $k_{\text{ph-nuc}} = c\sigma_{\text{ph-nuc}}n_{\text{air}} \approx 8 \times 10^2 \text{ s}^{-1}$, can be neglected in equation (2) as $k_{\text{ph-absorp}} \gg k_{\text{ph-nuc}}$. In Figure 2 one sees that the photon number $N_\gamma(t)$ (displayed as diamonds) first increases, as the TGF beam creates also secondary photons, which are counted in the simulation, but equation (2) approximates only the number of high-energy photons (with energies say $\gtrsim 1$ MeV), see further discussion by Rutjes et al. (2016).

The photonuclear cross section for nitrogen and for photons between 10 and 30 MeV ranges from 1 mb to a peak value of 14 mb at photon energy of 23 MeV (Obložinský, 2000). For the approximation of $k_{\text{ph-nuc}}$ above, we took the average photonuclear cross section of nitrogen $\sigma_{\text{ph-nuc}} \approx 2$ mb. The number of neutrons per TGF photon (between 10 MeV and 30 MeV) can then be approximated as $\frac{k_{\text{ph-nuc}}}{k_{\text{ph-absorp}}} \approx 4 \times 10^{-3}$ (consistent with the result of 4.3×10^{-3} by Babich et al., 2010). One may assume that all neutrons are generated—as this is limited by the photon absorption time scale $k_{\text{ph-absorp}}^{-1} \approx 5 \mu\text{s}$ —before they start to disappear by capture, which happens with a rate of $k_{\text{capt}} \approx (80 \text{ ms})^{-1}$ at 3 km altitude.

As already mentioned above k_{capt} does not depend on energy, but only on altitude. For the number of intermediate neutrons this yields

$$N_n(t) \approx N_\gamma(0) \frac{k_{\text{ph-nuc}}}{k_{\text{ph-absorp}}} \exp[-k_{\text{capt}} t] \quad \text{for } t \gg k_{\text{ph-absorp}}^{-1}. \quad (3)$$

This equation is consistent with our simulated neutron number, indicated with crosses in Figure 2 (bottom). For the gamma radiation of the TGF afterglow we need to use the number of neutrons and the reaction rate from the most significant pathway producing high-energy photons, that is, $n + {}^{14}\text{N} \rightarrow {}^{15}\text{N} + \gamma$, which happens with a rate of $k_{\text{n-ph}} = 0.7 \text{ s}^{-1}$ as the cross section equals $7.98 \times 10^{-30} \text{ m}^2$ (Choi et al., 2007) at thermal velocities (0.025 eV, 2200 m/s). Together this results in

$$N_{\gamma\text{-TGF afterglow}}(t) \approx \frac{k_{\text{n-ph}}}{k_{\text{ph-absorp}}} N_n(t) \approx N_\gamma(0) \frac{k_{\text{ph-nuc}} k_{\text{n-ph}}}{k_{\text{ph-absorp}}^2} \exp[-k_{\text{capt}} t] \quad \text{for } t \gg k_{\text{ph-absorp}}^{-1}. \quad (4)$$

where $\frac{k_{\text{ph-nuc}} k_{\text{n-ph}}}{k_{\text{ph-absorp}}^2} \approx 1.3 \times 10^{-8}$, consistent with our simulated photon numbers, indicated with diamonds in Figure 2 (bottom).

2.3. TGF Afterglow Generated by Neutrons (for Better Statistics)

The number of simulated photons in the TGF afterglow in Figure 2 is limited, as we started the Monte Carlo simulation with 10^8 primary photons, and as the conversion rate from photon to neutron and consecutively from neutron back to photon is low. To achieve better statistics, our second simulation starts directly with 10^8 neutrons at an altitude of 10 km. As photons with energies between 10 and 30 MeV are converted into neutrons with a probability of about 4×10^{-3} according to our calculations and to Babich et al. (2010), we have to multiply our simulation results for particle numbers now with a factor of $4 \times 10^{5 \pm 1}$ to simulate a TGF with $10^{16 \pm 1}$ primary photons in the required energy range.

The 10^8 neutrons of our simulation initially all have the most probable energy of 13 MeV, and they are directed downward, but they rapidly transit to isotropic diffusion. Figure 3 presents the evolution of neutrons and

photons in a similar manner as Figure 2, but now focused on the TGF afterglow after 1 ms. Apart from the better statistics of neutron to photon conversion, there are major differences to the earlier simulation. As the air density n_{air} is 2.2 times lower, the neutrons cool down 2.2 times more slowly, and they spread 2.2 times more widely; hence, the TGF afterglow is much more extended in space and duration. At the altitude of 10 km, it lasts for more than 1 s, as the rate constant k_{capt} in equation (3) is now $k_{\text{capt}} \approx 5 \text{ s}^{-1}$.

The statistics of Figure 3 are much better than those of Figure 2, but unfortunately the simulated box (see section 2.1) was too small to keep all particles. Figure 3 (top) clearly indicates that many particles leave the system at its upper border at 18 km altitude. Therefore, the normalization rates of equations (2)–(4) do not apply in the same fashion, so we rescaled them to fit the data. The decay rate of particles, however, with a rate constant of 5/s at 10 km altitude represents a good fit.

2.4. The Predicted Detector Signal

One question is whether the predicted TGF afterglow will be measurable above the cosmic background radiation. Figures 2 and 3 show that it will be hard to detect a TGF afterglow at sea level, if the neutrons are created above 3 km. We have calculated the predicted detector signal of the TGF afterglows for the simulation of Figure 2 at 3 km altitude and for the simulation of Figure 3 at 10 km altitude. The detector is the one of Gurevich et al. (2011) with an area of 475 cm^2 , and we used a temporal bin size of $200 \mu\text{s}$ as in their published plots. We assume that it is hit by $2 \text{ cm}^{-2} \text{ s}^{-1}$ or $9 \text{ cm}^{-2} \text{ s}^{-1}$ cosmic background photons with energy above our threshold of 10 keV at 3 or 10 km altitude, based on Bazilevskaya et al. (2008). This Poisson-distributed background is added to the signal in Figure 4.

As discussed above, the particle numbers of our simulation are orders of magnitude lower than those in a real TGF. The statistics of our simulation are corrected to 10^{16} initial photons between 10 and 30 MeV. Obviously, the TGF afterglow can clearly be detected above the cosmic background radiation. The signal would be even more conspicuous for TGFs containing 10^{17} or 10^{18} photon, above 10 MeV. It is important to remark that photons decay with a rate of $k_{\text{ph-absorp}} = (5 \mu\text{s})^{-1}$ at STP, or with $(7 \mu\text{s})^{-1}$ and $(15 \mu\text{s})^{-1}$ at 3 km and 10 km, respectively. Thus, the TGF signal from the simulation of Figure 2 is only visible as a point $t = 0 \text{ ms}$ in Figure 4, and the duration of the TGF afterglow is just the lifetime of the neutrons, as explained in equation (4).

2.5. Summary of Predictions for TGF Afterglows

We have predicted a new thunderstorm radiation mechanism, the TGF afterglow. It is formed by the photonuclear production of neutrons by the TGF, neutron propagation, and cooling and the inverse reaction that creates gamma rays again. TGF afterglows are thus a signature of gamma rays above 10 to 30 MeV. A TGF afterglow can be distinguished from TGFs or gamma ray glows by the following criteria:

1. *Duration.* A TGF lasts not longer than $200 \mu\text{s}$, or possibly $600 \mu\text{s}$ depending on the interpretation of some observations as one or several flashes. A gamma ray glow lasts for seconds or more, see Figure 1. A TGF afterglow lasts for 60 to 600 ms depending on the atmospheric altitudes crossed by the intermediate neutrons acting as their source, see equation (1). See also Figure 1 for illustration.
2. *Signal shape.* Neutron and photon signal appear suddenly and decay in time, compared to the photon and neutron signal in a gamma ray glow which first swells and then decays.
3. *Correlation with fast field changes.* TGF afterglows are created by TGFs which are triggered by leader propagation and related to fast electric field changes. Gamma ray glows are seen before a discharge and can be terminated by one.
4. *Photon isotropy.* The photons of a TGF afterglow are fairly isotropic, in contrast to the beams produced either in a TGF or in a gamma ray glow by the beamed motion of electrons and their beamed gamma ray emission by bremsstrahlung.
5. *Energy range.* The photon energy does not exceed the photon nuclear energy of $\epsilon_N \approx 10 \text{ MeV}$ for nitrogen, compared to many tens of MeV in a gamma ray glow or TGF.

3. Possible Observations and Outlook

As already mentioned in section 1, Gurevich et al. (2011) have reported gamma ray emissions lasting for 0.1 to 0.6 s. Clearly, the duration is significantly longer than any TGF detected or simulated, which should disappear within a millisecond, but the signals reported by Gurevich et al. (2011) are many orders longer. They occurred during the full duration of an atmospheric discharge at the Tien-Shan Cosmic Ray station at 3.3 to 3.9 km altitude, within the Tien-Shan mountains that reach up to almost 7.5 km altitude. Gurevich et al. (2011) found

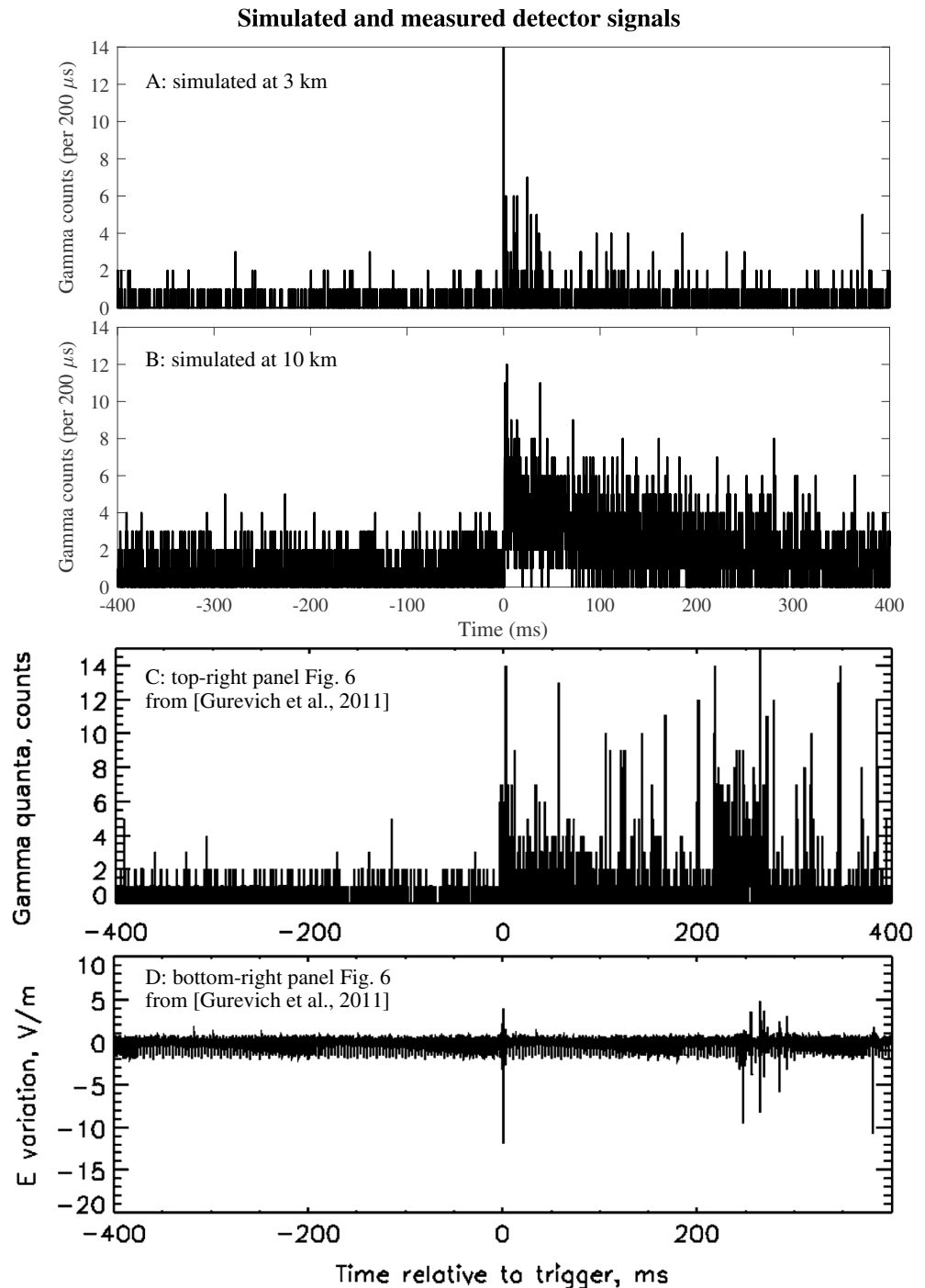


Figure 4. (a, b) Simulated counts of gamma radiation from the simulation presented in Figures 2 and 3. (c, d) Taken from Gurevich et al. (2011), in which it is denoted there as event “6.” Figures 4a to 4c are gamma ray counts per 200 μs interval on a detector of 475 cm^2 , at 3, 10, and 3.8 km, respectively. Figure 4d gives the measured fast electric field variation (20 μs sampling rate measured by the capacity sensor, see Gurevich et al., 2011 for more details).

that the temporal distribution of gamma radiation intensity in a burst is quite nonuniform, with some time structures on the scale of millisecond strongly correlated with an electric field change during the discharge. Based on duration only, the measurements fall in the regime of TGF afterglows, see Figure 1 for illustration.

To illustrate how TGF afterglows would qualitatively appear in measurements, we added one event from Gurevich et al. (2011) to Figures 4c and 4d. The measured gamma ray counts in Figure 4c appear suddenly at

$t = 0$ ms, simultaneous with a fast field variation given in Figure 4d, after which it decays in time. This measured structure in Figure 4c, from 0 ms to 200 ms, shows similarities to our simulated TGF afterglow at 3 km. But, the observations are probably not produced by the specific TGF that we simulated (a TGF starting at 8 km and directed vertically downward), there could be other scenarios (different altitude, orientation, opening angle, and photon spectrum); in addition, also the number of photons per TGF varies by an order of magnitude.

The measurements of Gurevich et al. (2011) show also structures that would not fit in the description of a TGF afterglow. Namely, structures that first swell and then decay, centered around one or multiple fast field variations. An example of such a structure is also seen in Figures 4c and 4d, between 200 ms and 300 ms. We speculate that it fits in the description of a gamma ray glow, but a transient one with a much shorter lifetime than typically measured. It could be the result of field development by previous partial discharges, producing a transient patch of air with an electric field above runaway breakdown, until the patch itself is discharged by a leader.

There may be more candidates of gamma ray observations from thunderstorms which are actually TGF afterglows. We have summarized discriminators in section 2.5 to search for TGF afterglows and we invite other researchers to look for their signatures in their millisecond time scale gamma ray measurements.

Acknowledgments

C. R. acknowledges funding by FOM project 12PR3041. G. D. is supported by the Brazilian agencies CAPES and CNPq. Data (e.g., cross sections) used in this work were provided by the software package FLUKA (see section 2.1) available at www.fluka.org.

References

- Adachi, T., Takahashi, Y., Ohya, H., Tsuchiya, F., Yamashita, K., Yamamoto, M., & Hashiguchi, H. (2008). Monitoring of lightning activity in Southeast Asia: Scientific objectives and strategies, Kyoto Working Papers on Area Studies: G-COE Series (Vol. 11). Center for Southeast Asian Studies, Kyoto University.
- Babich, L. (2007). Neutron generation mechanism correlated with lightning discharges. *Geomagnetism and Aeronomy*, *47*(5), 664–670.
- Babich, L. P. (2006). Generation of neutrons in giant upward atmospheric discharges. *JETP Letters*, *84*(6), 285–288.
- Babich, L. P., Bochkov, E. I., Kutsyk, I. M., & Rassoul, H. K. (2014). Analysis of fundamental interactions capable of producing neutrons in thunderstorms. *Physical Review D*, *89*, 093010. <https://doi.org/10.1103/PhysRevD.89.093010>
- Babich, L. P., Bochkov, E. I., Kutsyk, I. M., & Roussel-Dupré, R. A. (2010). Localization of the source of terrestrial neutron bursts detected in thunderstorm atmosphere. *Journal of Geophysical Research*, *115*, A00E28. <https://doi.org/10.1029/2009JA014750>
- Babich, L., Donskoy, E., Kutsyk, I., & Roussel-Dupré, R. (2005). The feedback mechanism of runaway air breakdown. *Geophysical Research Letters*, *32*, L09809. <https://doi.org/10.1029/2004GL021744>
- Babich, L. P., Kudryavtsev, A. Y., Kudryavtseva, M., & Kutsyk, I. (2007). Terrestrial gamma-ray flashes and neutron pulses from direct simulations of gigantic upward atmospheric discharge. *JETP Letters*, *85*(10), 483–487.
- Babich, L., Kudryavtsev, A. Y., Kudryavtseva, M., & Kutsyk, I. (2008). Atmospheric gamma-ray and neutron flashes. *Journal of Experimental and Theoretical Physics*, *106*(1), 65–76.
- Babich, L. P., & Roussel-Dupré, R. A. (2007). Origin of neutron flux increases observed in correlation with lightning. *Journal of Geophysical Research*, *112*, D13303. <https://doi.org/10.1029/2006JD008340>
- Bazilevskaya, G. A., Usoskin, I. G., Flückiger, E. O., Harrison, R. G., Desorgher, L., Bütikofer, R., ... Kovaltsov, G. A. (2008). Cosmic ray induced ion production in the atmosphere. *Space Science Reviews*, *137*, 149–173. <https://doi.org/10.1007/s11214-008-9339-y>
- Blatt, J. M., & Weisskopf, V. F. (1979). *Theoretical Nuclear physics*. New York: Springer-Verlag.
- Böhlen, T., Cerutti, F., Chin, M., Fassò, A., Ferrari, A., Ortega, P., ... Vlachoudis, V. (2014). The fluka code: Developments and challenges for high energy and medical applications. *Nuclear Data Sheets*, *120*, 211–214.
- Bratolyubova-Tsulukidze, L., Grachev, E., Grigoryan, O., Kunitsyn, V., Kuzhevskij, B., Lysakov, D., ... Usanova, M. (2004). Thunderstorms as the probable reason of high background neutron fluxes at $L < 1.2$. *Advances in Space Research*, *34*(8), 1815–1818.
- Briggs, M. S., Connaughton, V., Wilson-Hodge, C., Preece, R. D., Fishman, G. J., Kippen, R. M., ... Smith, D. M. (2011). Electron-positron beams from terrestrial lightning observed with Fermi GBM. *Geophysical Research Letters*, *38*, L02808. <https://doi.org/10.1029/2010GL046259>
- Briggs, M. S., Fishman, G. J., Connaughton, V., Bhat, P. N., Paciesas, W. S., Preece, R. D., ... Chekhtman, A. (2010). First results on terrestrial gamma ray flashes from the Fermi Gamma-ray Burst Monitor. *Journal of Geophysical Research*, *115*, A07323. <https://doi.org/10.1029/2009JA015242>
- Carlson, B., Lehtinen, N. G., & Inan, U. S. (2010). Neutron production in terrestrial gamma ray flashes. *Journal of Geophysical Research*, *115*, A00E19. <https://doi.org/10.1029/2009JA014696>
- Celestin, S., & Pasko, V. P. (2011). Energy and fluxes of thermal runaway electrons produced by exponential growth of streamers during the stepping of lightning leaders and in transient luminous events. *Journal of Geophysical Research*, *116*, A03315. <https://doi.org/10.1029/2010JA016260>
- Celestin, S., Xu, W., & Pasko, V. P. (2012). Terrestrial gamma ray flashes with energies up to 100 MeV produced by nonequilibrium acceleration of electrons in lightning. *Journal of Geophysical Research*, *117*, A05315. <https://doi.org/10.1029/2012JA017535>
- Chanrion, O., Bonaventura, Z., Çinar, D., Bourdon, A., & Neubert, T. (2014). Runaway electrons from a “beam-bulk” model of streamer: Application to TGFs. *Environmental Research Letters*, *9*, 55,003. <https://doi.org/10.1088/1748-9326/9/5/055003>
- Chanrion, O., & Neubert, T. (2010). Production of runaway electrons by negative streamer discharges. *Journal of Geophysical Research*, *115*, A00E32. <https://doi.org/10.1029/2009JA014774>
- Chilingarian, A., Bostanjyan, N., & Vanyan, L. (2012). Neutron bursts associated with thunderstorms. *Physical Review D*, *85*(8), 085017.
- Chilingarian, A., Daryan, A., Arakelyan, K., Hovhannisyanyan, A., Mailyan, B., Melkumyan, L., ... Vanyan, L. (2010). Ground-based observations of thunderstorm-correlated fluxes of high-energy electrons, gamma rays, and neutrons. *Physical Review D*, *82*(4), 043009.
- Chilingarian, A., Hovsepian, G., & Hovhannisyanyan, A. (2011). Particle bursts from thunderclouds: Natural particle accelerators above our heads. *Physical Review D*, *83*(6), 062001.
- Chilingarian, A., Hovsepian, G., Khanikyan, G., Reymers, A., & Soghomonian, S. (2015). Lightning origination and thunderstorm ground enhancements terminated by the lightning flash. *EPL (Europhysics Letters)*, *110*(4), 49001.
- Choi, H., Firestone, R., Lindstrom, R., Molnár, G. L., Mughabghab, S., Revay, Z., ... Zhou, C. (2007). *Database of Prompt Gamma Rays from Slow Neutron Capture for Elemental Analysis*. Vienna: International Atomic Energy Agency.

- Cooray, V., Arevalo, L., Rahman, M., Dwyer, J., & Rassoul, H. (2009). On the possible origin of X-rays in long laboratory sparks. *Journal of Atmospheric and Solar-Terrestrial Physics*, 71(17), 1890–1898.
- Dietrich, S. S., & Berman, B. L. (1988). Atlas of photoneutron cross sections obtained with monoenergetic photons. *Atomic Data and Nuclear Data Tables*, 38(2), 199–338.
- Drozdov, A., Grigoriev, A., & Malyshev, Y. (2013). Assessment of thunderstorm neutron radiation environment at altitudes of aviation flights. *Journal of Geophysical Research: Space Physics*, 118, 947–955. <https://doi.org/10.1029/2012JA018302>
- Dwyer, J. (2003). A fundamental limit on electric fields in air. *Geophysical Research Letter*, 30(20), 2055. <https://doi.org/10.1029/2003GL017781>
- Dwyer, J. R. (2007). Relativistic breakdown in planetary atmospheres. *Physics of Plasmas (1994–present)*, 14(4), 042901.
- Dwyer, J. R. (2012). The relativistic feedback discharge model of terrestrial gamma ray flashes. *Journal of Geophysical Research*, 117, A02308. <https://doi.org/10.1029/2011JA017160>
- Dwyer, J. R., Grefenstette, B. W., & Smith, D. M. (2008). High-energy electron beams launched into space by thunderstorms. *Geophysical Research Letters*, 35, L02815. <https://doi.org/10.1029/2007GL032430>
- Dwyer, J., Saleh, Z., Rassoul, H., Concha, D., Rahman, M., Cooray, V., ... Rakov, V. (2008). A study of X-ray emission from laboratory sparks in air at atmospheric pressure. *Journal of Geophysical Research: Atmospheres*, 113, D23207. <https://doi.org/10.1029/2008JD010315>
- Eack, K. B., Beasley, W. H., Rust, W. D., Marshall, T. C., & Stolzenburg, M. (1996). Initial results from simultaneous observation of X-rays and electric fields in a thunderstorm. *Journal of Geophysical Research*, 101(D23), 29,637–29,640.
- Ferrari, A., Sala, P. R., Fasso, A., & Ranft, J. (2005). Fluka: A multi-particle transport code (program version 2005) (Tech. Rep). Geneva: CERN.
- Fishman, G. J., Bhat, P., Malozzi, R., Horack, J., Koshut, T., Kouveliotou, C., ... Christian, H. J. (1994). Discovery of intense gamma-ray flashes of atmospheric origin. *Science*, 264(5163), 1313–1316.
- Fleischer, R. L., Plumer, J., & Crouch, K. (1974). Are neutrons generated by lightning?. *Journal of Geophysical Research*, 79(33), 5013–5017.
- Gjesteland, T., Østgaard, N., Laviola, S., Miglietta, M., Arnone, E., Marisaldi, M., ... Montanya, J. (2015). Observation of intrinsically bright terrestrial gamma ray flashes from the Mediterranean basin. *Journal of Geophysical Research: Atmospheres*, 120, 12,143–12,156. <https://doi.org/10.1002/2015JD023704>
- Gurevich, A. (1961). On the theory of runaway electrons. *Soviet Physics JETP*, 12(5), 904–912.
- Gurevich, A., Antonova, V., Chubenko, A., Karashtin, A., Kryakunova, O., Lutsenko, V. Y., ... Zybin, K. P. (2015). The time structure of neutron emission during atmospheric discharge. *Atmospheric Research*, 164, 339–346.
- Gurevich, A., Antonova, V., Chubenko, A., Karashtin, A., Mitko, G., Ptitsyn, M., ... Zybin, K. P. (2012). Strong flux of low-energy neutrons produced by thunderstorms. *Physical Review Letters*, 108(12), 125001.
- Gurevich, A., Chubenko, A., Karashtin, A., Mitko, G., Naumov, A., Ptitsyn, M., ... Zybin, K. P. (2011). Gamma-ray emission from thunderstorm discharges. *Physics Letters A*, 375(15), 1619–1625.
- Gurevich, A., Milikh, G., & Roussel-Dupre, R. (1992). Runaway electron mechanism of air breakdown and preconditioning during a thunderstorm. *Physics Letters A*, 165(5), 463–468.
- Kelley, N. A., Smith, D. M., Dwyer, J. R., Splitt, M., Lazarus, S., Martinez-McKinney, F., ... Rassoul, H. K. (2015). Relativistic electron avalanches as a thunderstorm discharge competing with lightning. *Nature Communications*, 6, 7845.
- Kochkin, P., Köhn, C., Ebert, U., & van Deursen, L. (2016). Analyzing X-ray emissions from meter-scale negative discharges in ambient air. *Plasma Sources Science and Technology*, 25(4), 044002.
- Kochkin, P., Nguyen, C., Van Deursen, A., & Ebert, U. (2012). Experimental study of hard X-rays emitted from metre-scale positive discharges in air. *Journal of Physics D: Applied Physics*, 45(42), 425202.
- Kochkin, P., Van Deursen, A., & Ebert, U. (2015). Experimental study on hard X-rays emitted from metre-scale negative discharges in air. *Journal of Physics D: Applied Physics*, 48(2), 25205.
- Köhn, C., Chanrion, O., & Neubert, T. (2016). The influence of bremsstrahlung on electric discharge streamers in N₂, O₂ gas mixtures. *Plasma Sources Science and Technology*, 26(1), 15,006.
- Köhn, C., & Ebert, U. (2015). Calculation of beams of positrons, neutrons, and protons associated with terrestrial gamma ray flashes. *Journal of Geophysical Research: Atmospheres*, 120, 1620–1635. <https://doi.org/10.1002/2014JD022229>
- Köhn, C., Ebert, U., & Mangiarotti, A. (2014). The importance of electron-electron bremsstrahlung for terrestrial gamma-ray flashes, electron beams and electron-positron beams. *Journal of Physics D: Applied Physics*, 47(25), 252,001.
- Kostyrya, I., Tarasenko, V., Tkachev, A., & Yakovlenko, S. (2006). X-ray radiation due to nanosecond volume discharges in air under atmospheric pressure. *Technical Physics*, 51(3), 356–361.
- Kozlov, V., Mullayarov, V., Starodubtsev, S., & Toropov, A. (2013). Neutron bursts during cloud-to-ground discharges of lightning. *Bulletin of the Russian Academy of Sciences: Physics*, 77(5), 584–586.
- Li, C., Ebert, U., & Hundsdorfer, W. (2009). 3D hybrid computations for streamer discharges and production of runaway electrons. *Journal of Physics D: Applied Physics*, 42(20), 202,003.
- Mailyan, B., Briggs, M., Cramer, E., Fitzpatrick, G., Roberts, O., Stanbro, M., ... Dwyer, J. (2016). The spectroscopy of individual terrestrial gamma-ray flashes: Constraining the source properties. *Journal of Geophysical Research: Space Physics*, 121, 11,346–11,363. <https://doi.org/10.1002/2016JA022702>
- Marisaldi, M., Fuschino, F., Pittori, C., Verrecchia, F., Giommi, P., Tavani, M., ... Trois, A. (2014). The first AGILE low-energy (<30 MeV) terrestrial gamma-ray flashes catalog. *EGU General Assembly 2014, held 27 April - 2 May, 2014 in Vienna, Austria, id.11326*.
- McCarthy, M., & Parks, G. (1985). Further observations of X-rays inside thunderstorms. *Geophysical Research Letters*, 12(6), 393–396.
- Moss, G. D., Pasko, V. P., Liu, N., & Veronis, G. (2006). Monte Carlo model for analysis of thermal runaway electrons in streamer tips in transient luminous events and streamer zones of lightning leaders. *Journal of Geophysical Research*, 111, A02307. <https://doi.org/10.1029/2005JA011350>
- Nguyen, C. V., van Deursen, A. P., & Ebert, U. (2008). Multiple X-ray bursts from long discharges in air. *Journal of Physics D: Applied Physics*, 41(23), 234,012.
- Noggle, R., Krider, E., & Wayland, J. (1968). A search for X-rays from helium and air discharges at atmospheric pressure. *Journal of Applied Physics*, 39(10), 4746–4748.
- Oblozinsky, P. (2000). Handbook of photonuclear data for applications: Cross sections and spectra (report IAEA-TECDOC-1178). Vienna Austria: International Atomic Energy Association.
- Rep'ev, A., & Repin, P. (2008). Spatiotemporal parameters of the X-ray radiation from a diffuse atmospheric-pressure discharge. *Technical Physics*, 53(1), 73–80.
- Rutjes, C., Sarria, D., Skeltved, A. B., Luque, A., Diniz, G., Østgaard, N., & Ebert, U. (2016). Evaluation of Monte Carlo tools for high energy atmospheric physics. *Geoscientific Model Development*, 9(11), 3961–3974.
- Shah, G., Razdan, H., Bhat, C., & Ali, Q. (1985). Neutron generation in lightning bolts. *Nature*, 313, 773–775.

- Shao, T., Zhang, C., Niu, Z., Yan, P., Tarasenko, V. F., Baksht, E. K., ... Shutko, Y. V. (2011). Diffuse discharge, runaway electron, and x-ray in atmospheric pressure air in an inhomogeneous electrical field in repetitive pulsed modes. *Applied Physics Letters*, *98*(2), 21,503.
- Shyam, A., & Kaushik, T. (1999). Observation of neutron bursts associated with atmospheric lightning discharge. *Journal of Geophysical Research*, *104*(A4), 6867–6869.
- Stankevich, Y. L., & Kalinin, V. (1967). Fast electrons and X radiation during the initial stages of an impulse spark discharge in air. *Doklady Akademii Nauk SSSR*, *177*(Nov.-Dec. 1967), 72–73.
- Starodubtsev, S. A., Kozlov, V., Toropov, A., Mullayarov, V., Grigor'ev, V. G., & Moiseev, A. (2012). First experimental observations of neutron bursts under thunderstorm clouds near sea level. *JETP Letters*, *96*(3), 188–191.
- Tarasenko, V. F., Baksht, E. K., Burachenko, A. G., Kostyrya, I. D., Lomaev, M. I., & Rybka, D. V. (2008). Generation of supershort avalanche electron beams and formation of diffuse discharges in different gases at high pressure. *Plasma Devices and Operations*, *16*(4), 267–298.
- Torii, T., Takeishi, M., & Hosono, T. (2002). Observation of gamma-ray dose increase associated with winter thunderstorm and lightning activity. *Journal of Geophysical Research*, *107*(D17), 4324. <https://doi.org/10.1029/2001JD000938>
- Toropov, A., Kozlov, V., Mullayarov, V., & Starodubtsev, S. (2013). Experimental observations of strengthening the neutron flux during negative lightning discharges of thunderclouds with tripolar configuration. *Journal of Atmospheric and Solar-Terrestrial Physics*, *94*, 13–18.
- Tsuchiya, H., Enoto, T., Yamada, S., Yuasa, T., Kawaharada, M., Kitaguchi, T., ... Makishima, K. (2007). Detection of high-energy gamma rays from winter thunderclouds. *Physical Review Letters*, *99*(16), 165,002.